

A conserved regulatory mode in exocytic membrane fusion revealed by Mso1p membrane interactions

Marion Weber-Boyvot^{a,b,*}, Hongxia Zhao^{a,*}, Nina Aro^{a,c}, Qiang Yuan^a, Konstantin Chernov^a, Johan Peränen^a, Pekka Lappalainen^a, and Jussi Jääntti^{a,c}

^aCell and Molecular Biology Program, Institute of Biotechnology, FI-00014 University of Helsinki, Finland; ^bMinerva Foundation Institute for Medical Research, FI-00290 Helsinki, Finland; ^cVTT Technical Research Centre of Finland, FI-02044 VTT, Finland

ABSTRACT Sec1/Munc18 family proteins are important components of soluble N-ethylmaleimide-sensitive factor attachment protein receptor (SNARE) complex-mediated membrane fusion processes. However, the molecular interactions and the mechanisms involved in Sec1p/Munc18 control and SNARE complex assembly are not well understood. We provide evidence that Mso1p, a Sec1p- and Sec4p-binding protein, interacts with membranes to regulate membrane fusion. We identify two membrane-binding sites on Mso1p. The N-terminal region inserts into the lipid bilayer and appears to interact with the plasma membrane, whereas the C-terminal region of the protein binds phospholipids mainly through electrostatic interactions and may associate with secretory vesicles. The Mso1p membrane interactions are essential for correct subcellular localization of Mso1p–Sec1p complexes and for membrane fusion in *Saccharomyces cerevisiae*. These characteristics are conserved in the phosphotyrosine-binding (PTB) domain of β -amyloid precursor protein-binding Mint1, the mammalian homologue of Mso1p. Both Mint1 PTB domain and Mso1p induce vesicle aggregation/clustering in vitro, supporting a role in a membrane-associated process. The results identify Mso1p as a novel lipid-interacting protein in the SNARE complex assembly machinery. Furthermore, our data suggest that a general mode of interaction, consisting of a lipid-binding protein, a Rab family GTPase, and a Sec1/Munc18 family protein, is important in all SNARE-mediated membrane fusion events.

Monitoring Editor

Thomas F. J. Martin
University of Wisconsin

Received: May 31, 2012

Revised: Oct 26, 2012

Accepted: Nov 20, 2012

INTRODUCTION

A complex molecular machinery regulates intracellular transport vesicle targeting, tethering, and fusion at the plasma membrane. Vesicle tethering by the exocyst complex leads to a cascade in which vesicle

and plasma membrane-anchored Q- and R-soluble N-ethylmaleimide-sensitive factor attachment protein receptor (SNARE) proteins pair and assemble into SNARE complexes (Jahn and Scheller, 2006). After tethering, a sequence of events involving the Rab GTPase Sec4p, Sec1p, SNAREs, and several other proteins takes place (He and Guo, 2009; Hutagalung and Novick, 2011). In *Saccharomyces cerevisiae* Sec1p, a member of the Sec1p/Munc18 (SM) protein family, is essential for the exocytic SNARE-mediated membrane fusion (Toonen and Verhage, 2003; Kauppi et al., 2004; Carr and Rizo, 2010). How all these components cooperate to achieve efficient and timely membrane fusion and exocytosis is unclear.

So far, only a few non-SNARE SM-binding proteins have been identified. In mammalian cells, Mint1, Mint2, Doc2, granulophilin/Slp4, and phospholipase D interact with Munc18 (Okamoto and Sudhof, 1997; Verhage et al., 1997; Lee et al., 2004). In yeast, Mso1p cooperates with Sec1p in exocytosis (Aalto et al., 1997; Knop et al., 2005; Weber et al., 2010), Vac1p with Vps45p in vacuole maintenance (Weisman and Wickner, 1992), and Ily1p with Vps33p in

This article was published online ahead of print in MBoC in Press (<http://www.molbiolcell.org/cgi/doi/10.1091/mbc.E12-05-0415>) on November 28, 2012.

*These authors contributed equally.

Address correspondence to: Jussi Jääntti (jussi.jaantti@vtt.fi).

Abbreviations used: APP, β -amyloid precursor protein; BiFC, bimolecular fluorescence complementation; DPH, 1,6-diphenyl-1,3,5-hexatriene; POPC, 1-palmitoyl-2-oleoyl-sn-glycero-3-phosphatidylcholine; POPE, 1-palmitoyl-2-oleoyl-sn-glycero-3-phosphatidylethanolamine; POPS, 1-palmitoyl-2-oleoyl-sn-glycero-3-phosphatidylserine; PTB, phosphotyrosine binding; SNARE, soluble N-ethylmaleimide-sensitive factor attachment protein receptor.

© 2013 Weber-Boyvot et al. This article is distributed by The American Society for Cell Biology under license from the author(s). Two months after publication it is available to the public under an Attribution-Noncommercial-Share Alike 3.0 Unported Creative Commons License (<http://creativecommons.org/licenses/by-nc-sa/3.0>).

"ASCB®," "The American Society for Cell Biology®," and "Molecular Biology of the Cell®" are registered trademarks of The American Society of Cell Biology.

endosomal membrane fusion (Lazar *et al.*, 2002). In addition, Sec6p, a subunit of the exocyst tethering complex, was recently shown to interact with Sec1p (Morgera *et al.*, 2012).

Deletion of *MSO1* causes vesicle accumulation at the site of exocytosis and inhibition of vesicle fusion during the de novo plasma membrane formation in meiotic diploid yeast cells (Aalto *et al.*, 1997; Jantti *et al.*, 2002; Knop *et al.*, 2005). In addition to Sec1p binding, Mso1p cooperates with the Rab GTPase Sec4p in exocytosis (Castillo-Flores *et al.*, 2005; Knop *et al.*, 2005; Weber-Boyvatt *et al.*, 2011). Mso1p is homologous to the phosphotyrosine-binding (PTB) domain of the mammalian SM-interacting protein Mint1, which in addition to the PTB domain has a separate Munc18-interacting domain and two PDZ domains (Knop *et al.*, 2005). Mint proteins have been proposed to act as adaptors for the molecular machinery involved in neuronal exocytosis (Okamoto and Sudhof, 1997). Mint1 interacts with phosphoinositides and the β -amyloid precursor protein (APP) through its PTB domain (Okamoto and Sudhof, 1997). The APP interaction is implicated in amyloid production and ultimately Alzheimer's disease development (Rogelj *et al.*, 2006; Ho *et al.*, 2008).

In this study we show that Mso1p is a novel membrane-interacting protein. We show that this property of Mso1p is important for its in vivo function and is conserved in its mammalian homologue Mint1 PTB domain. Taken together, our results reveal a novel membrane interaction mode for a Sec1p-binding protein and suggest the existence of a conserved set of molecular interactions that are involved in the assembly of SNARE complexes in general.

RESULTS

Mso1p interacts with phosphatidylinositol (4,5)-bisphosphate-rich membranes in yeast cells

The molecular mechanisms required for proper SNARE complex assembly are not well understood. The Mint1 PTB domain, the mammalian Mso1p homologue, binds phosphoinositides with a preference for phosphatidylinositol (4,5)-bisphosphate (PI(4,5)P₂; Okamoto and Sudhof, 1997). However, the exact mechanism and the physiological role of this interaction are not known. This prompted us to examine the possible membrane interaction of yeast Mso1p and to elucidate physiological consequences of this interaction.

First, the in vivo Ras-rescue assay (Isakoff *et al.*, 1998) was applied to evaluate membrane interactions of Mso1p. This method scores for proteins that can target a constitutively active Ras1Q61L to the plasma membrane at the restrictive temperature in *cdc25ts* mutant cells. Full-length Mso1p fused to Ras1pQ61L rescued the growth of *cdc25ts* cells at 37°C at comparable level to a well-characterized plasma membrane-interacting PH domain of PLC γ (Figure 1A). The analysis of different Mso1p fragments revealed that the N-terminal amino acids 1–39 were sufficient for plasma membrane targeting (Figure 1A). Our previous results showed that residues 1–39 are not involved in Mso1p binding to the plasma membrane-associated Sec1p or the syntaxin homologues Sso1/2p (Weber *et al.*, 2010). Thus the Ras-rescue assay results suggest that the N-terminal region of Mso1p interacts with the plasma membrane.

The plasma membrane is enriched with PI(4,5)P₂, and this lipid is a known binding partner for many plasma membrane-associated proteins (Di Paolo and De Camilli, 2006; Mayinger, 2012). We therefore tested the possible contribution of PI(4,5)P₂ to localization of Mso1p–Sec1p complexes. In temperature-sensitive phosphatidylinositol-4-phosphate 5-kinase *mss4ts* mutant cells the PI(4,5)P₂ levels are reduced by 49% at the permissive temperature (24°C) and by 83% at the restrictive temperature (37°C; Stefan *et al.*, 2002). The *mss4ts* and wild-type cells were transformed with plasmids express-

ing *YFP(C)-MSO1* and *SEC1-Venus(N)* and subjected to analysis using the bimolecular fluorescence complementation (BiFC) assay (Hu *et al.*, 2002; Skarp *et al.*, 2008; Weber *et al.*, 2010). In *mss4ts* cells, Mso1p–Sec1p BiFC signal persisted at the permissive temperature 24°C but was partially mislocalized along the plasma membrane (Supplemental Figure S1, A and B). At restrictive temperature the polarized BiFC signal was lost in the bud in 52% of the cells (Supplemental Figure S1, A and B). Thus, whereas the plasma membrane association of the Mso1p–Sec1p complex was not significantly affected by diminished PI(4,5)P₂ levels, the polarized localization of the complex was disrupted upon PI(4,5)P₂ depletion. These data suggest that Mso1p can interact with the plasma membrane through its N-terminal region and that PI(4,5)P₂ levels may play a role in modulating the distribution of Mso1p–Sec1p complexes at the plasma membrane.

Mso1p interacts with phosphoinositide-rich membranes in vitro

To examine whether Mso1p interacts directly with membranes, we carried out in vitro vesicle cosedimentation assays using purified recombinant full-length Mso1p and different Mso1p fragments. The full-length Mso1p and the N- and C-terminal fragments (residues 1–39 and 40–210, respectively) cosedimented efficiently with both zwitterionic and negatively charged vesicles (Figure 1B and Supplemental Figure S2), displaying similar binding to the different phosphoinositides tested. Thus we chose to use a lipid composition (POPC:POPE:POPS:PIP₂ = 50:20:20:10, where POPC is 1-palmitoyl-2-oleoyl-*sn*-glycero-3-phosphatidylcholine, POPE is 1-palmitoyl-2-oleoyl-*sn*-glycero-3-phosphatidylethanolamine, POPS is 1-palmitoyl-2-oleoyl-*sn*-glycero-3-phosphatidylserine, and PIP₂ is phosphatidylinositol (4,5)-bisphosphate) resembling that of the plasma membrane as a representative model system for the subsequent assays. The affinity of the full-length Mso1p for PI(4,5)P₂-rich membranes was similar to the I-BAR domain of MIM (Figure 1B), which binds phosphoinositide-rich membranes with high affinity (Saarikangas *et al.*, 2009). The affinities of the N- and C-terminal Mso1p fragments to membranes were weaker compared with the I-BAR domain but stronger compared with cofilin-1 (Figure 1B), which is a highly conserved actin and PIP₂-binding protein (Zhao *et al.*, 2010).

The lipid binding of Mso1p C-terminus was clearly salt dependent (residues 40–210; Figure 1C). In contrast, the membrane binding of the full-length Mso1p was only mildly salt dependent, and the N-terminal fragment (residues 1–39) showed negligible salt dependence. These results suggest that the C-terminal fragment of Mso1p interacts with membranes predominantly through electrostatic interactions, whereas the N-terminus binds to the membranes mainly through hydrophobic interactions.

To examine whether the hydrophobic interaction of the Mso1p N-terminal fragment involves penetration into the lipid bilayer, we examined the effect of this lipid-binding motif on membrane fluidity by steady-state 1,6-diphenyl-1,3,5-hexatriene (DPH) anisotropy (Saarikangas *et al.*, 2009). The DPH anisotropy increased significantly after the vesicles were incubated with purified full-length Mso1p (Figure 1D), suggesting that Mso1p not only binds, but also inserts into a lipid bilayer. It is important to note that although the membrane-binding affinity of Mso1p was not significantly affected by phosphoinositides (Supplemental Figure S2), membrane penetration of Mso1p was enhanced by phosphatidylinositol 3,5-bisphosphate, PI(4,5)P₂, and phosphatidylinositol (3,4,5)-trisphosphate (PI(3,4,5)P₃; Figure 1D). To identify the membrane penetration motif of Mso1p, we measured the DPH anisotropy with various Mso1p

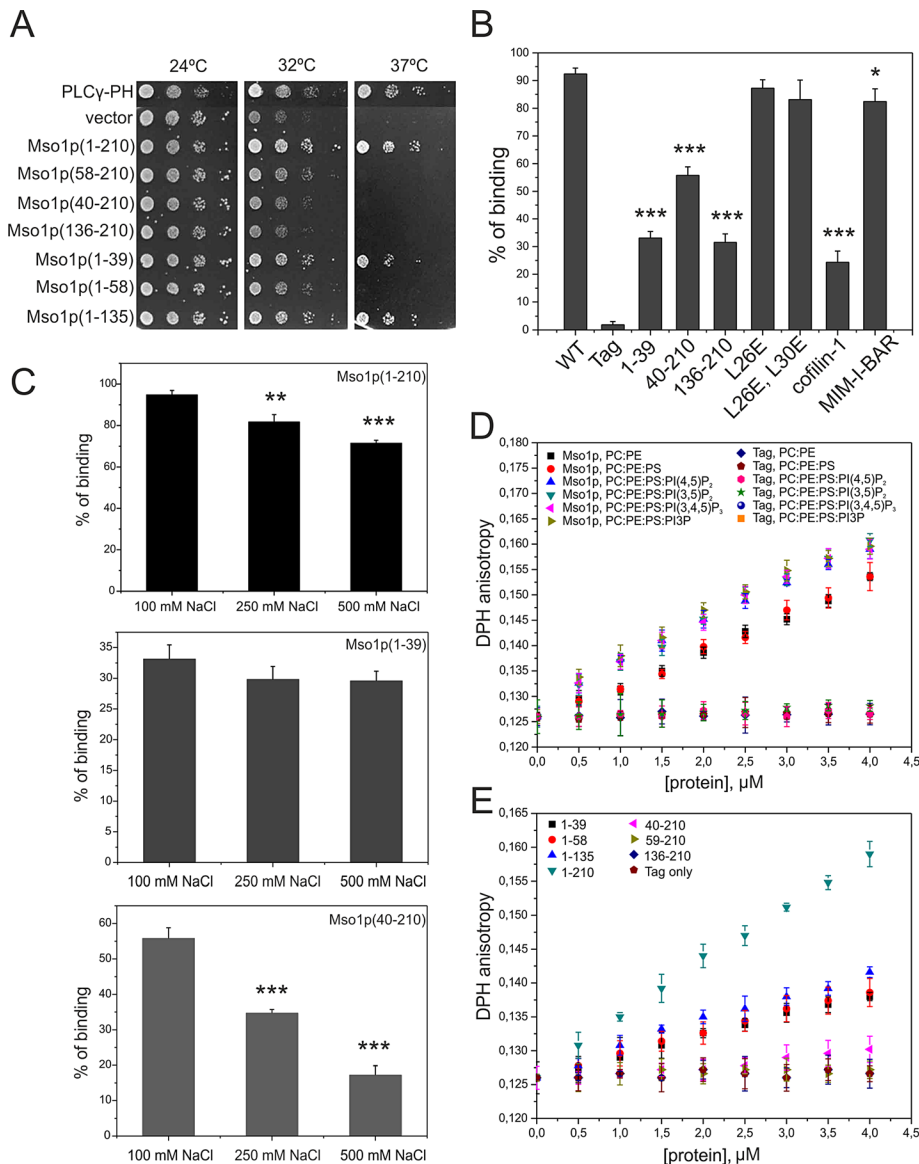


FIGURE 1: Mso1p interacts with membranes through two distinct binding sites. (A) Mapping of the Mso1p membrane interaction domain in vivo. The growth of *cdc25ts* mutant cells transformed with plasmids expressing different Mso1p fragments fused to RasQ61L. RasQ61L fused to PLC γ -PH was used as a positive control. (B) Vesicle cosedimentation assay of Mso1p with PI(4,5)P₂-rich membranes. Mso1p binds to the PI(4,5)P₂-rich membrane with a high affinity, similar to the well-known membrane-binding protein MIM I-BAR. The Mso1p fragments lacking either the N-terminus or the C-terminus displayed weaker cosedimentation with vesicles and bound membranes with similar affinity to a known actin/lipid-binding protein, cofilin-1. The point mutations disrupting the amphipathic properties of the N-terminal helix of Mso1p did not significantly affect the membrane-binding affinity. The lipid composition was POPC:POPE:POPS:PIP₂ = 50:20:20:10. The final concentrations of proteins and lipids were 3 and 500 μ M, respectively. Error bars represent SD. Student's *t* test, **p* < 0.05 and ****p* < 0.001. (C) The salt dependence of Mso1p cosedimented with PIP₂-containing vesicles. The membrane binding of Mso1p C-terminus was salt dependent (residues 40–210). In contrast, the membrane binding of the full-length Mso1p was only mildly affected by salt, and the N-terminal fragment (residues 1–39) showed negligible salt dependence. Student's *t* test, ***p* < 0.01 and ****p* < 0.001. (D) The effect of Mso1p on lipid bilayer fluidity as measured by DPH anisotropy. Mso1p increased the DPH anisotropy in both zwitterionic and negatively charged membranes, whereas the tag alone did not display detectable effects on DPH anisotropy. Phosphoinositides enhanced the effects of Mso1p on the changes of membrane fluidity. The lipid composition is indicated in the figure, and the total lipid concentration was 40 μ M. For PC:PE and PC:PE:PS membranes the compositions were 80:20 and 60:20:20, respectively. (E) The effect of Mso1p fragments on membrane fluidity in the DPH anisotropy assay. The Mso1p fragments lacking the C-terminus of the protein displayed reduced effects on DPH anisotropy. However, the mutants

fragments (Figure 1E). The data revealed that the first 39 amino acids are sufficient and necessary for membrane insertion in vitro (Figure 1E). However, the effect of the N-terminal Mso1p fragment (residues 1–39) on membrane fluidity was reduced by ~50% compared with the full-length protein, suggesting that the attachment of the Mso1p C-terminal region to the membrane surface through electrostatic interactions may facilitate the membrane insertion of the N-terminus.

The membrane insertion of Mso1p and its penetration depth were measured by analyzing the quenching efficiency for the intrinsic Trp fluorescence by lipids that are brominated at different positions along the acyl chain. Because the DPH anisotropy suggested that Mso1p inserts into the lipid bilayer through the N-terminal 1–39 amino acids, we monitored the fluorescence quenching of Trp-16 to measure its membrane penetration. Based on the quenching data, the insertion depth of Trp-16 in the full-length Mso1p and in the N-terminal (1–39) fragment was estimated to be ~9.55 Å from the center of the lipid bilayer (Supplemental Figure S3). Taken together, these data show that Mso1p binds phosphoinositide-rich membranes with high affinity through two biochemically distinct sites. The N-terminal region can insert into the lipid bilayer and binds membranes mainly through hydrophobic interactions, whereas the C-terminal region applies electrostatic interactions to bind phosphoinositide-rich membranes.

Conserved leucines are important for the membrane insertion of Mso1p and the Mint1 PTB domain

The N-terminal fragment of Mso1p contains several hydrophobic residues that might contribute to membrane insertion. Especially leucine 26 is well conserved in the mammalian Mso1p homologue, the Mint1 PTB domain (Zhang *et al.*, 1997), this residue is located in an accessible loop distinct from the amyloid precursor peptide-binding site (Figure 2A). The contribution of Mso1p leucines 26 and 30 to membrane insertion was examined after mutating these residues to glutamates in order to disrupt the amphipathic properties

lacking the N-terminal region of the protein completely lost the ability to increase DPH anisotropy, suggesting that the N-terminal region is important for membrane insertion and the C-terminal region of Mso1p facilitates the membrane insertion. The lipid composition used was POPC:POPE:POPS:PI(4,5)P₂ = 50:20:20:10.

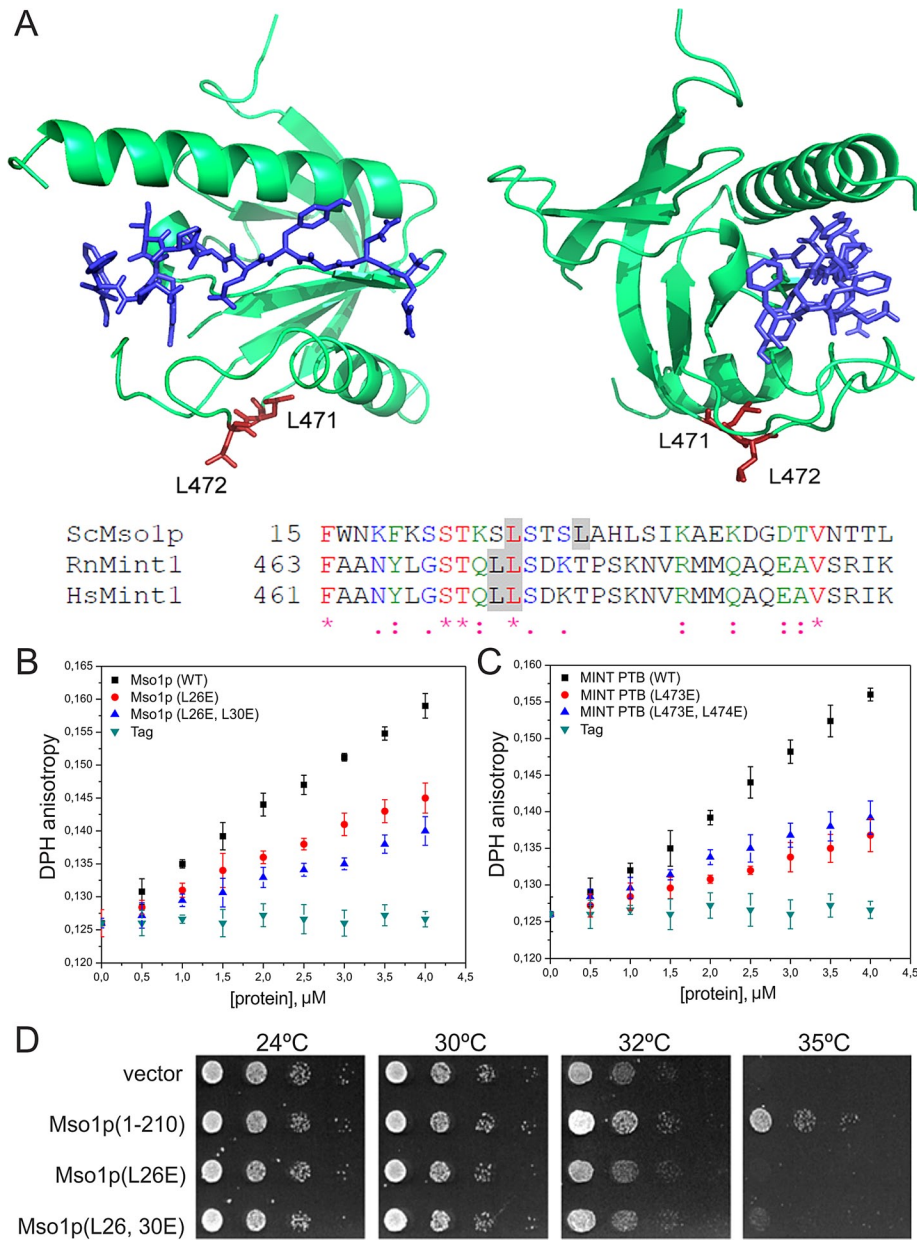


FIGURE 2: The membrane insertion mode is conserved between Mso1p and the mammalian Mint1 PTB domain. (A) Two views of the crystal structure (PDB 1x11; Zhang *et al.* 1997) of human Mint1 PTB domain and a sequence comparison of Mso1p N-terminus with human and rat Mint1 PTB domain. Asterisk, identical; colon, strongly similar; and period, similar amino acids. The gray shading highlights the mutated amino acids. The conserved amino acids are labeled in the structure. The PTB domain-bound APP peptide is shown in blue. (B) The effects of Mso1p point mutations (L26E and L26,30E) on DPH anisotropy. These mutants displayed reduced effects on DPH anisotropy compared with the wild-type protein, suggesting the importance of these leucine residues in membrane penetration. Lipid composition of membranes used was POPC:POPE:POPS:PIP2 = 50:20:20:10. (C) The effects of the rat Mint1 PTB domain on membrane fluidity. Similar to Mso1p, the Mint PTB domain significantly increased the DPH anisotropy, suggesting that it inserts into the lipid bilayer. Furthermore, the mutations in conserved leucines (L473,474E) resulted in diminished effects on DPH anisotropy, providing further evidence for the importance of these leucines in membrane penetration. Lipid composition was as in B. (D) The growth of *cdc25ts*-mutant cells transformed with plasmids expressing indicated Mso1p mutants fused to RasQ61L.

of the N-terminal helix of Mso1p. Circular dichroism spectroscopy analysis provided evidence that these mutations did not disrupt the folding of Mso1p (Supplemental Figure S4). Compared to the

formation (Figure 3C). At the same time cells expressing *mso1(40-210)* displayed small, dispersed, cytosolic dotty structures that did not grow in size even after prolonged incubation. Bright-field light

wild-type Mso1p, the effects of L26E and L26,30E mutants on DHP anisotropy were significantly weaker, providing further evidence that the N-terminal region of Mso1p inserts into the lipid bilayer (Figure 2B). Furthermore, similar to the corresponding Mso1p residues, mutations in leucines 473 and 474 in rat Mint1 resulted in a reduced effect on DHP anisotropy (Figure 2C). This suggests that these amino acids in the Mint1 PTB domain contributed to membrane insertion. These data show that Mint1 PTB inserts into the lipid bilayer and that the mode of membrane interaction for Mso1p and Mint1 PTB appears to be conserved. In line with the *in vitro* results, Mso1p (L26E) and Mso1p (L26,30E) did not rescue the temperature-sensitive growth of *cdc25* cells in the Ras-rescue assay (Figure 2D).

Mso1p membrane insertion is needed for the correct subcellular localization of Mso1p–Sec1p complexes and for membrane fusion *in vivo*

The contribution of Mso1p membrane bilayer insertion to the localization of Mso1p–Sec1p complexes was investigated using the BiFC assay (Hu *et al.*, 2002). Wild-type cells were transformed with plasmids expressing *SEC1-Venus(N)* and different *YFP(C)-MSO1* constructs. For Mso1p(1–210) and Mso1p(1–135) a fluorescence signal was observed at the plasma membrane of growing buds (Figure 3A). The signal was cytosolic in cells expressing Mso1p(40–210), Mso1p(L26E), and Mso1p(L26,30E). This suggests that in these mutants the formation of Mso1p–Sec1p complexes persisted, yet their localization to the plasma membrane was compromised without a fully active Mso1p lipid insertion motif. In line with the previous results, no BiFC signal was obtained for Mso1p(1–39) and Mso1p(136–210), which lack the Sec1p-binding domain (Knop *et al.*, 2005; Weber *et al.*, 2010).

Mso1p is essential for the homotypic vesicle fusion during prospore membrane formation in meiotic diploid cells (Knop *et al.*, 2005). Homozygous *mso1(40-210)/mso1(40-210)* cells expressing *mso1(40-210)* as the sole copy of *MSO1* under its own promoter did not sporulate (Figure 3B). Don1p is a marker protein for the leading-edge membrane of the prospore membrane during its growth around the haploid nucleus (Knop and Strasser, 2000). In cells expressing the wild-type *MSO1*, elongated Don1–green fluorescent protein (GFP)–positive structures were observed at early time points of spore formation (Figure 3C). At the same time cells expressing *mso1(40-210)* displayed small, dispersed, cytosolic dotty structures that did not grow in size even after prolonged incubation. Bright-field light

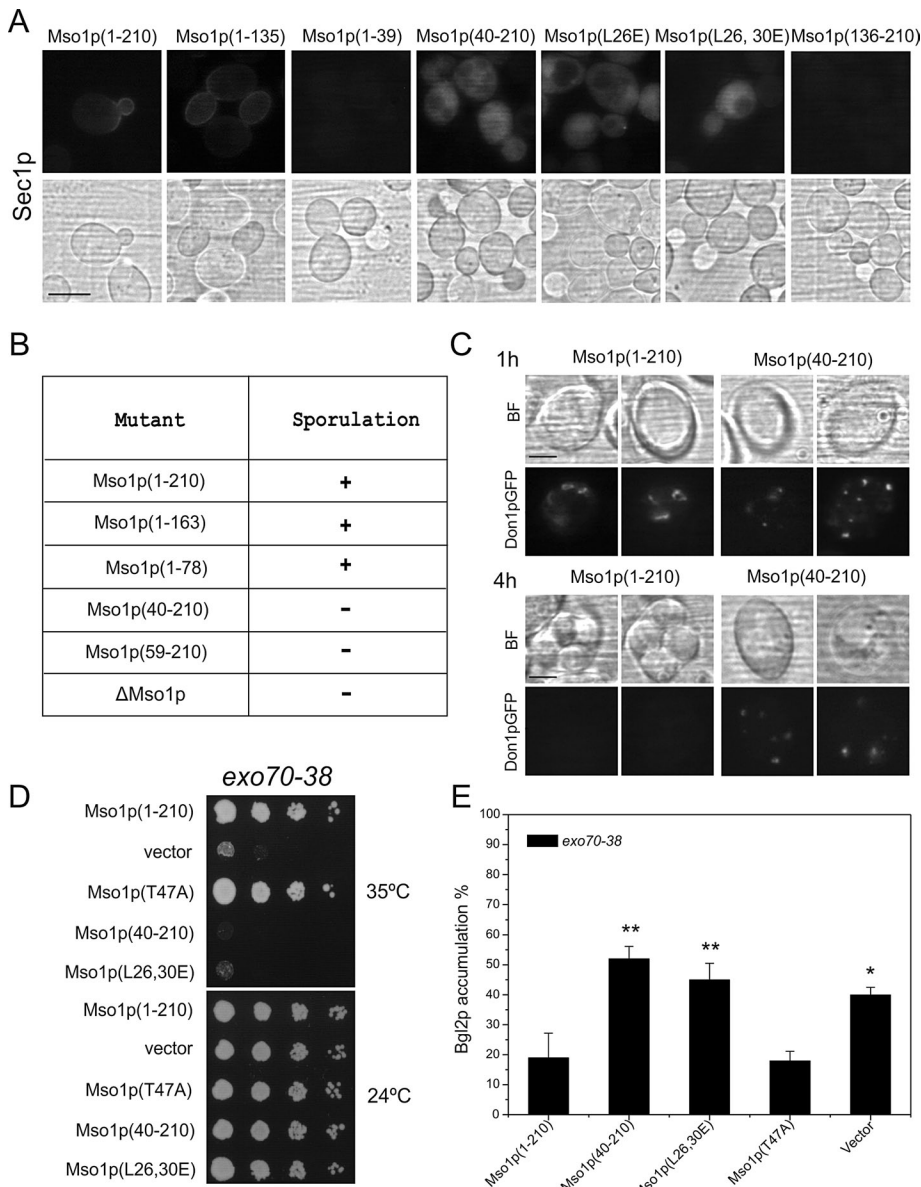


FIGURE 3: The N-terminus is important for Mso1p *in vivo* function. (A) Localization of the Mso1p–Sec1p BiFC signal *in vivo*. Haploid, vegetatively grown wild-type cells (H304) coexpressing the indicated YFP(C)-tagged Mso1p variants with Sec1p-Venus(N) investigated by fluorescence microscopy. Scale bar, 5 μ m. (B) The sporulation ability of cells expressing different Mso1p mutants. (C) Localization of Don1p-GFP and spore formation in *MSO1* wild-type and *mso1(40-210)* diploid cells. Scale bar, 2 μ m. (D) Mso1p N-terminus is required for multicopy suppression of the temperature-sensitive growth of *exo70-38* cells. *exo70-38* (H3742) cells were transformed with plasmids expressing different versions of Mso1p, followed by monitoring of cell growth at indicated temperatures. (E) Mso1p membrane insertion is functionally important for protein secretion in *exo70-38* cells. Bgl2p accumulation was measured by Western blotting from lysates prepared from *exo70-38* cells grown at 37°C expressing different versions of Mso1p. Error bars represent SD (minimum of three independent experiments). Student's *t* test, **p* < 0.05 and ***p* < 0.01.

microscopy showed that no spores formed in these cells, whereas in wild-type cells the spores matured and Don1-GFP detached from the membrane (Figure 3C, 4-h time point). These results suggest that membrane insertion by the N-terminus is required for the homotypic membrane fusion of the prospore membrane precursor vesicles.

Recently novel temperature-sensitive mutants were generated for Exo70, an exocyst complex subunit that interacts with the plasma

membrane through PI(4,5)P₂ binding (He *et al.*, 2007b). *MSO1* overexpression suppressed the temperature-sensitive growth of *exo70-38* cells (Figure 3D). This activity required the first 39 amino acids of Mso1p and was affected by L26,30E mutations. At the same time, this genetic link was not affected by the T47A mutation, which abolishes Mso1p interaction with Sec1p (Knop *et al.*, 2005). To assess the functional contribution of the Mso1p lipid binding in protein secretion, we analyzed the secretion capacity of *exo70-38* cells when the cells were overexpressing different mutant variants of Mso1p. A clear intracellular accumulation of endo- β -1,3-glucanase Bgl2p, a secretory protein, was observed in *exo70-38* cells at the restrictive temperature (Figure 3E, vector). This accumulation was rescued by overexpression of the full-length Mso1p or the Sec1p binding-deficient mutant Mso1pT47A. However, no rescue for Bgl2p accumulation was observed in cells expressing *mso1(40-210)* or *mso1(L26,30E)* mutants.

The Mso1p N-terminus is closely associated with the plasma membrane, whereas the C-terminus colocalizes with Sec4p on intracellular membranes

The contribution of the Mso1p N-terminal region to plasma membrane targeting was tested by coexpression of full-length Mso1p (1–210) with different Mso1p mutants in the BiFC assay. A fluorescence signal was obtained for full-length Mso1p in combination with Mso1p (1–210, 1–135, and 1–39), suggesting a close proximity at the plasma membrane (Figure 4A). In line with the Ras-rescue assay results, no signal was obtained for the full-length Mso1p with L26E and L26,30E mutants or 40–210 and 136–210 fragments.

Mso1p interacts with the GTP-bound Sec4p *in vitro*, and BiFC analysis suggests that the interaction site resides in mobile intracellular membranes in close proximity to the plasma membrane (Weber-Boyvat *et al.*, 2011). Different Mso1p membrane interaction mutants were tested for their proximity to Sec4p(Q79L), the GTP bound form of Sec4p. In line with previous work (Weber-Boyvat *et al.*, 2011), full-length Mso1p resulted in a signal with Sec4p(Q79L) at intracellular membrane elements in the bud (Figure 4B). Of importance, this signal

was not significantly affected by deletion of the N-terminal membrane-inserting region or L26,30E mutations. These results suggest that the Mso1p N-terminal membrane-insertion motif could mediate interactions with the plasma membrane, whereas the C-terminus of Mso1p could reside in close proximity to Sec4p in intracellular vesicular membranes. However, the results do not show whether these interactions occur separately or if they can coincide.

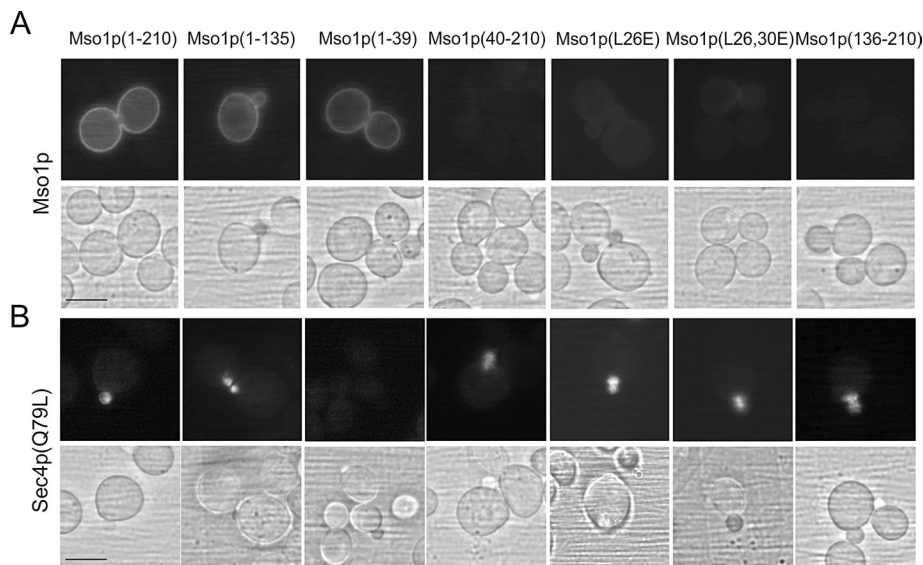


FIGURE 4: The contribution of the Mso1p N- and C-terminal domains to the localization of the BiFC signal for Mso1p–Mso1p and Mso1p–Sec4pQ79L protein pairs in vivo. Haploid, vegetatively grown cells (H304) expressing YFP(C)-tagged Mso1p variants with (A) Mso1p–YFP(N) or (B) YFP(N)Sec4p(Q79L) were investigated by fluorescence microscopy. Scale bar, 5 μ m.

The lipid interactions of Mint1 PTB domain contribute to plasma membrane localization of Mint1–Munc18 protein complexes in mammalian cells

The *in vitro* data (Figure 2) suggested that Mso1p and the Mint1 PTB domain share features that enable them to interact with membranes. To address the possible *in vivo* role of the Mint1 membrane interaction, we assessed the contribution of PTB domain in membrane targeting in mammalian neuron-like PC6.3 cells. To achieve this, we analyzed the interaction site for the full-length rat Mint1 and rat Sec1 orthologue Munc18-1 by fluorescence microscopy. Unstimulated PC6.3 cells display a roundish morphology with short membrane protrusions (Figure 5A). In these cells Mint1–Munc18 protein pairs were observed concentrated in the protrusions by BiFC. When different fragments of Mint1 were subjected to the same analysis it was observed that the introduction of L473E and L474E mutation into the PTB domain reduced the localization of the Mint1–Munc18 pairs at the cell protrusions (Figure 5, B and C). Similar level of reduction was observed when the C-terminal PDZ domains were deleted from Mint1 (Munc18-binding domain [MID] + PTB; Figure 5, B and C). When L473E and L474E mutations were introduced into this N-terminal part of Mint1 (MID+PTB L473E L474E) an additional reduction in the localization of Mint1–Munc18 in the cell protrusions was observed. When the MID was coexpressed with Munc18 the BiFC signal was almost completely lost at the plasma membrane and instead signal in the cytosol was observed to increase. In line with previous results (Okamoto and Sudhof, 1997), the coexpression of just the PTB domain with Munc18 did not result in a fluorescence signal in the BiFC assay. These findings suggest an important role for the Mint1 PTB domain and the conserved leucine residues for targeting of Mint1–Munc18 complexes to cell protrusions in PC6.3 cells.

Colocalization of the Mint1–Munc18 BiFC interaction site with sole Mint1 and Munc18 showed that whereas Munc18 alone displayed a rather strong cytosolic localization, Mint1 colocalized predominantly with the Mint1–Munc18 BiFC at the protrusions (Figure 5D). This finding led us to compare the mCherry-Mint1 localization to the localization of PI(3,4)P₂ (visualized by GFP-PKB α PH domain),

PI(4,5)P₂ (visualized by GFP-PLC δ PH domain), and PI(3,4,5)P₃ (visualized by GFP-GRP1 PH domain). A significant colocalization of Mint1 with PI(3,4)P₂ and PI(3,4,5)P₃ in the cell protrusions was observed in PC6.3 cells (Figure 5E). At the same time PI(4,5)P₂ appeared to generally label the plasma membrane. Taken together, the results suggest that Mint1 PTB domain coincides with PI species *in vivo* and that this binding may contribute to the localization of Mint1–Munc18 BiFC complexes.

Mso1p and Mint1 PTB domains induce vesicle aggregation in vitro

The existence of N- and C-terminal membrane interaction domains raised the possibility that Mso1p could use them to mediate binding between, for example, secretory vesicles and the plasma membrane. The ability to interlink membranes was tested using an *in vitro* vesicle-clustering assay. In the assay light scattering is recorded in a solution containing membrane vesicles and the purified recombinant wild-type or mutant

proteins. Addition of the full-length Mso1p (0.5 μ M) induced significant increase in light scattering, suggesting a strong vesicle clustering (Figure 6A). Of importance, this property of Mso1p was dependent on the two independent lipid-binding sites because the Mso1p fragments Mso1p(40–210), Mso1p(1–39), and Mso1p(136–210), devoid of either membrane-binding site, caused only weak or nondetectable effects of light scattering (Figure 6, A and B). Furthermore, the L26E and L26,30E mutations, which displayed moderate defects in lipid bilayer insertion (Figure 2B), also reduced the vesicle clustering as detected by a light scattering assay (Figure 6A). Of interest, similar to Mso1p, Mint1 PTB domain-induced vesicle aggregation/clustering was diminished in mutants, which affected the membrane insertion activity of the domain (Figure 6, C and D).

DISCUSSION

The molecular cascade that leads from transport vesicle tethering to membrane fusion is composed of a series of well-orchestrated molecular interactions that ensure that transport vesicles with cargo and destination determinants fuse with the correct target membrane. The assembly of SNARE complex components has been studied extensively, and purified SNARE complex subunits can spontaneously assemble even *in vitro* (Sollner *et al.*, 1993). However, the molecular mechanisms that prevent spontaneous SNARE complex assembly *in vivo* are still poorly understood. These mechanisms are likely to involve a “proofreading” system in the form of ordered, stepwise molecular interactions that ensure that only correct SNARE complexes are formed *in vivo*. This “proofreading” system is a prerequisite for the maintenance of the compartmentalized organization of the exocytic and endocytic membrane compartments in eukaryotic cells.

Several small GTP-binding proteins regulate the functionality of the exocyst tethering complex in exocytosis (Hutagalung and Novick, 2011). These interactions involve hydrolysis of GTP and are likely to ensure directionality in the assembly and/or conformational changes in the exocyst before and during the tethering process. The exocyst subunits Sec3p and Exo70p have been shown to bind phosphoinositide lipids, and this binding contributes to

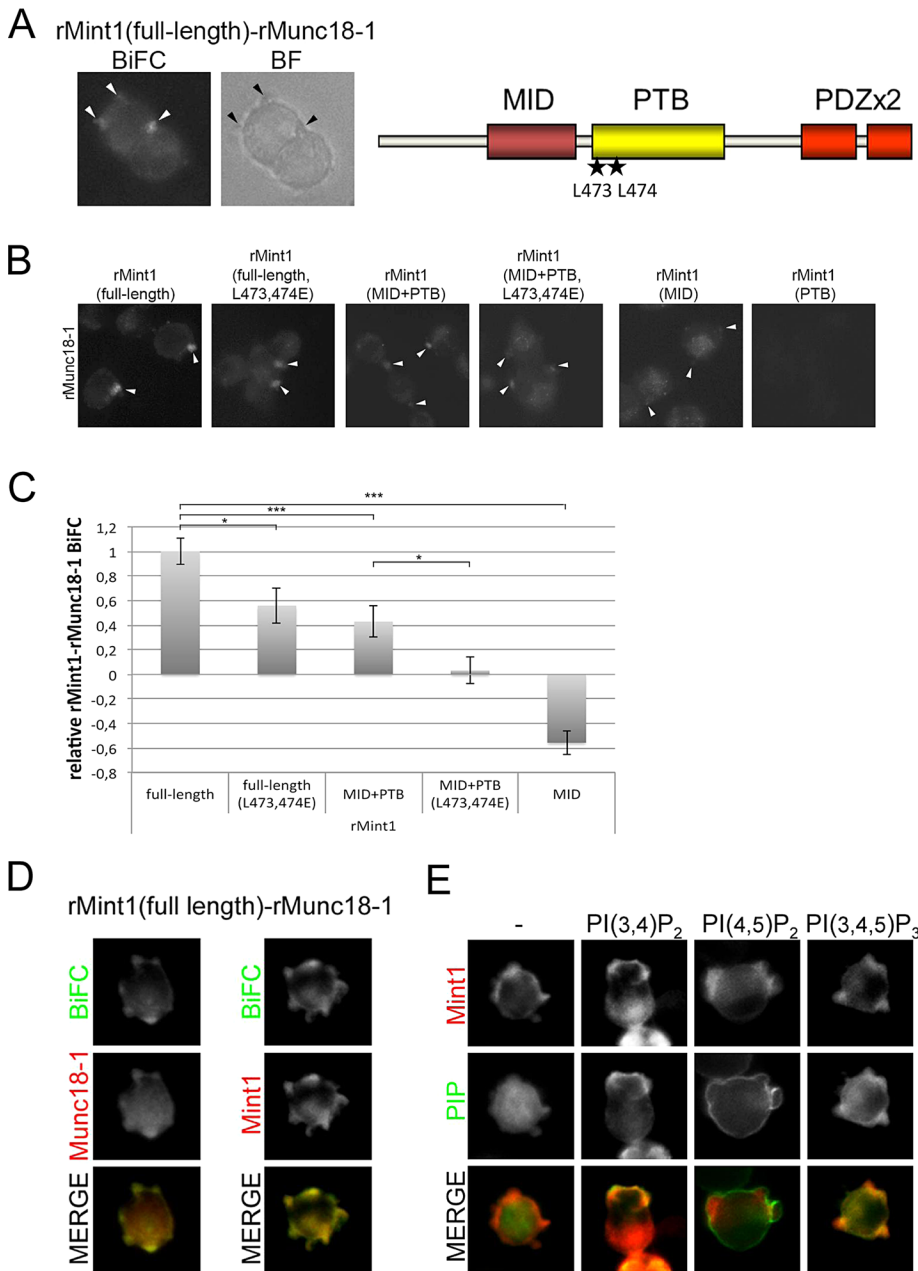


FIGURE 5: Mint1 PTB domain–lipid interactions contribute to plasma membrane localization of Mint1–Munc18 protein complexes in neuron-like mammalian PC6.3 cells. (A) rMunc18-1 interacts with rMint1 at cell protrusions. Fluorescence imaging of cells transfected with plasmids expressing rMunc18-1–Venus(N) and Venus(C)-rMint1. Right, schematic presentation of the domain structure of Mint1. The localizations of L473 and L474 are indicated by stars in the PTB domain. MID, Munc18-binding domain; PDZ, PSD95/Dlg1/ZO-1-domain; PTB, phosphotyrosine-binding domain. (B) The rMint1 lipid interaction contributes to rMunc18-1–rMint1 BiFC localization at cell protrusions. Fluorescence imaging of cells transfected with plasmids expressing rMunc18-1–Venus(N) and Venus(C)-rMint1 (full-length, full-length L473,474E, MID+PTB, MID+PTB L473,474E, MID, and PTB). (C) Quantification of B. The intensity of the BiFC signal at the protrusions was analyzed in a minimum of 25 cells per interaction mode and normalized to the cytosolic BiFC signal of the same cell. Error bars are SEM (SE of the mean). Student's *t* test, **p* < 0.05 and ****p* < 0.001. (D) mCherry-rMint1 colocalizes with rMint1–rMunc18-1 BiFC complexes. Fluorescence imaging of PC6.3 cells transfected with plasmids expressing rMunc18-1–Venus(N), Venus(C)-rMint1, and mCherry-rMunc18-1 or mCherry-rMint1. (E) rMint1 localizes to PI(3,4)P₂- and PI(3,4,5)P₃-positive cell protrusions. Fluorescence imaging of PC6.3 cells transfected with plasmids expressing mCherry-rMint1 and GFP-tagged PLCδ PH domain(R40L) (–; a non-PIP-binding negative control), PKBα PH domain (PI(3,4)P₂), PLCδ PH domain (PI(4,5)P₂), or GRP1 PH domain (PI(3,4,5)P₃).

in vivo functionality of these proteins (He *et al.*, 2007b; Zhang *et al.*, 2008). Recently additional physical links between the exocyst and the SNARE complex were suggested by the findings showing binding of the exocyst subunit Sec6p with the SNARE complex subunit Sec9p and with the SNARE complex-binding protein Sec1p (Sivaram *et al.*, 2006; Morgera *et al.*, 2012). Additional support for the functional linkage between the exocyst and Sec1p is provided by genetics and immunoprecipitation experiments (Wiederkehr *et al.*, 2004). It is likely that there are still several unidentified auxiliary proteins that contribute to the SNARE complex assembly in vivo. Furthermore, it is evident that even for many of the already known components the molecular details for their function are poorly understood.

We previously identified Mso1p as a Sec1p-binding protein that in addition can physically interact with a GTP-bound Sec4p Rab GTPase (Weber-Boyvat *et al.*, 2011). The PTB domain of mammalian Sec1p-binding protein Mint1, the putative mammalian homologue of Mso1p, has been shown to bind phosphoinositides (Okamoto and Sudhof, 1997). This prompted us to test possible lipid interactions of Mso1p. Of interest, both in vivo and in vitro experiments indicate that Mso1p possesses two separate lipid interaction domains—one at the very N-terminus and a second one at the C-terminal region.

The two lipid-interacting regions display apparently different binding modes. The N-terminus is capable of inserting into the lipid bilayer and plays a role in Mso1p–plasma membrane interaction. The C-terminal region appears to bind membranes through electrostatic interactions and can reside in close proximity to the Rab GTPase Sec4p in intracellular membranes. The fact that the lipid-binding affinities of Mso1p are similar to those of the well-characterized lipid-binding protein MIM-I-BAR (Figure 1B) suggested that Mso1p–lipid interactions have significant in vivo consequences. We previously showed that Mso1p is essential for the prospore formation and thus sporulation of diploid *S. cerevisiae* cells (Knop *et al.*, 2005). Support for an in vivo role for the Mso1p lipid binding came from experiments showing that diploid cells that express as their sole copy of Mso1p a Mso1p mutant lacking the first 39 N-terminal amino acids did not sporulate.

It has been shown that Exo70 binds phosphoinositides at the plasma membrane (He *et al.*, 2007b). Mutations in the temperature-sensitive *exo70-38* allele cause

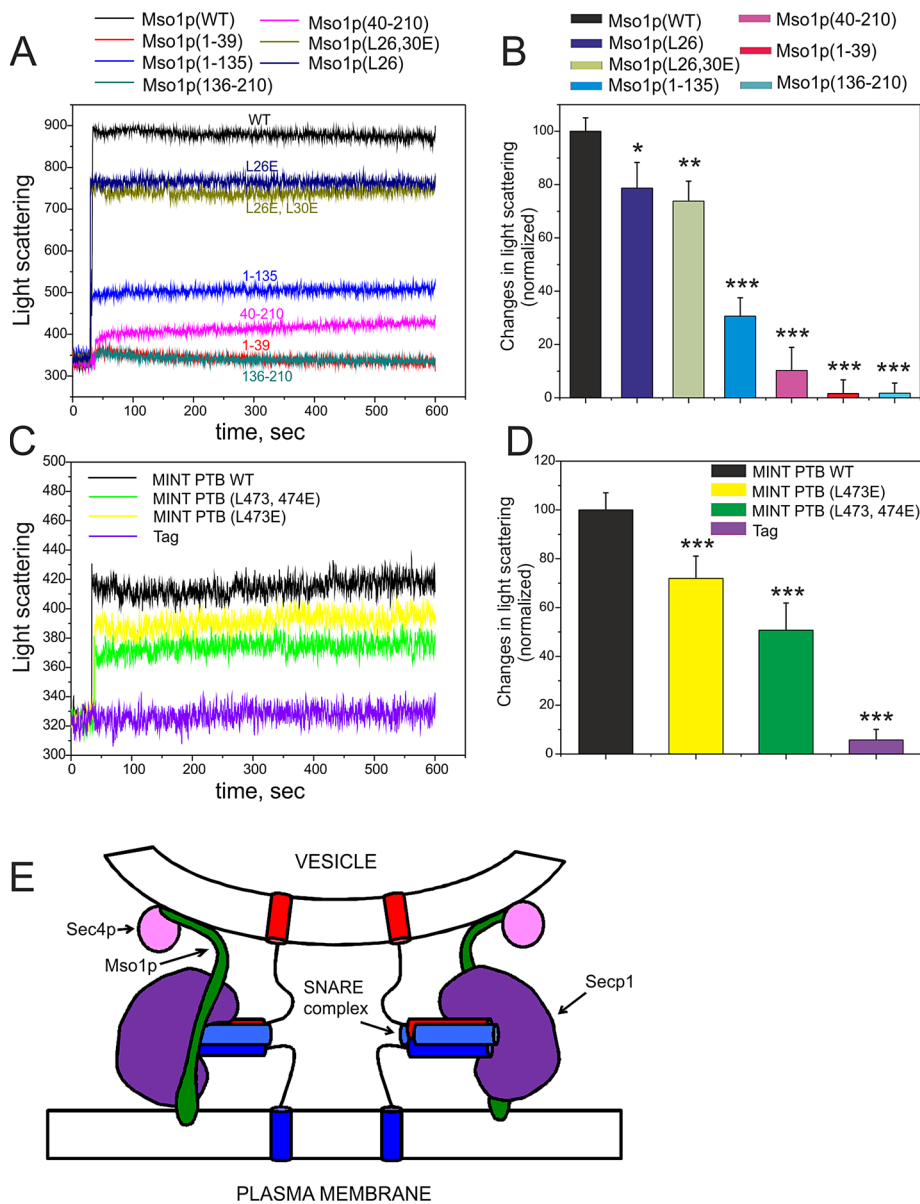


FIGURE 6: Mso1p and the Mint1 PTB domain can cluster PI(4,5)P₂-containing liposomes in vitro. (A) Mso1p caused significant increment in light scattering when added to liposome samples, suggesting that the protein can induce vesicle aggregation/clustering. In contrast, mutants lacking either N- or C-terminal regions or containing L26E and L26,30E mutations displayed weaker effects on light scattering, indicating that both membrane-binding sites are required for vesicle aggregation/clustering by Mso1p. (B) Quantification of light scattering data from three independent measurements at 500-s time point after addition of the protein. The assay was performed as described in *Materials and Methods*. Error bars represent SD. Student's *t* test, **p* < 0.05, ***p* < 0.01, and ****p* < 0.001. (C) Light scattering caused by the rat Mint1 PTB domain. Similar to Mso1p, the Mint1 PTB domain increases the light scattering of vesicles, and mutations of the conserved leucines (L473E and L474E) displayed weaker effects on light scattering. (D) Quantification of light scattering from three independent measurements at 500-s time point after addition of the protein. Student's *t* test, **p* < 0.05, ***p* < 0.01, and ****p* < 0.001. (E) A schematic presentation of known Mso1p interactions in the exocytic process. The depicted interactions of Mso1p with Sec1p, Sec4p, SNARE complex, and the membranes do not necessarily take place simultaneously in vivo. For more a more detailed description, see the text.

functional inactivation of Exo70p and intracellular accumulation of Bgl2p (He *et al.*, 2007a). Overexpression of the lipid-binding Mso1p could rescue both the temperature-sensitive growth and Bgl2p accumulation in *exo70-38* cells. These results support a positive role for Mso1p in stabilizing the exocytic protein machinery in vivo.

sight, for example, into the reported role of Mint1 in β -amyloid precursor protein generation.

S. cerevisiae has four SM family proteins: Sec1p, Vps33p, Vps45, and Sly1p (Toonen and Verhage, 2003). There is increasing evidence that the assembly process for fusion-competent SNARE complexes

Our in vitro experiments using light scattering suggest that Mso1p can induce vesicle clustering and that this activity is strongly dependent on both N- and C-terminal membrane-binding regions of Mso1p. This, together with our in vivo data, suggests that Mso1p possesses properties that would enable it to function, for example, as a linker between the Sec4p-containing intracellular membranes and the plasma membrane. Figure 6E shows the known Mso1p interactions. It was previously shown that Mso1p binds the Sec1p domain 1 (Weber *et al.*, 2010). This binding is mediated by amino acids 40–80 of Mso1p. Mso1p can interact with GTP-bound Sec4p, and this interaction is likely to use amino acids located in Mso1p(135–201) (Weber-Boyvatt *et al.*, 2011). It is possible and even likely that these interactions do not take place simultaneously in vivo. Nevertheless, the observed interactions suggest that Mso1p provides binding affinities for the multiprotein complex that is involved in membrane fusion regulation. We speculate that during this process Mso1p may interact with both the transport vesicle membrane and the plasma membrane. However, further studies are needed to reveal whether this binding can occur simultaneously and Mso1p can promote tethering of heterotypic membranes in vivo. Furthermore, novel technological approaches will be needed to gain full understanding of the detailed molecular interactions, the dynamics, and the order of events that take place in the exocytosis process.

Our results show that mutations in conserved hydrophobic amino acids in the Mint1 PTB domain affect its membrane interactions in vitro. In addition, these mutations also affect the localization of Mint1–Munc18 protein complexes (as analyzed by BiFC) to cell protrusions in mammalian neuron-like PC6.3 cells. It therefore appears that Mso1p membrane interaction properties are shared by the Mint1 PTB domain both in vitro and in vivo. Previous studies showed that Mint1 PTB domain binds phosphoinositols with a preference for PI(4,5)P₂ (Okamoto and Sudhof, 1997). Our results suggest that, in addition to the previously identified PI binding, the Mint PTB domain may possess a second, previously uncharacterized membrane insertion mode, similar to Mso1p. The identification and characterization of this site may in the future provide insight

involves sequential protein interactions, which are often of low affinity (Munson and Bryant, 2009; Carr and Rizo, 2010). The interactions revealed here identify a novel layer of regulation for the exocytic SNARE complex assembly that is likely to contribute to the stability and directionality of the molecular cascade leading to SNARE complex assembly. It is interesting to note that Mso1p interactions with Sec1p, the Rab GTPase Sec4p, and lipids resemble those of Vac1p and Ivy1p. Previous studies showed that, in addition to phosphoinositide binding, both Vac1p and Ivy1p interact with SM proteins Vps45p and Vps33p and the GTPases Vps21p and Ypt7p, respectively (Peterson et al., 1999; Tall et al., 1999; Lazar et al., 2002). Our results, combined with the aforementioned molecular interactions of Vps45p and Vps33p, suggest that there is a general requirement for a membrane-interacting adaptor protein for SM protein-mediated membrane fusion events in *S. cerevisiae*. We propose that the lipid interaction modes characterized here for Mso1p reveal a conserved pattern in the exocytic SNARE complex assembly pathway that is shared by all SNARE complexes. Although currently unidentified, our results suggest that such an adaptor protein may also exist for the yeast SM protein Sly1p. Furthermore, given our results on Mint1 and the high overall conservation in the molecular mechanisms of membrane fusion, it may well be that this type of molecular interaction mode is conserved from yeast to mammalian cells.

MATERIALS AND METHODS

Strains and plasmids

The yeast strains and plasmids used are shown in Supplemental Table S1. Yeast cells were grown as described previously (Sherman, 1991). Plasmids were generated by standard molecular biology techniques. Details on construction are available upon request. Point mutations were introduced using QuikChange (Promega, Madison, WI).

Fluorescence microscopy

Cells were grown to an OD₆₀₀ of 0.8–1 at the permissive temperature (24°C) in SC-Ura-Leu or SC-Ura-Leu-Trp medium. For the Mso1p–Mso1p BiFC experiments the yellow fluorescent protein (YFP)–Mso1p constructs were induced on medium lacking methionine for 4 h before examination in the microscope. In the case of temperature-sensitive strains, cells were shifted to the restrictive temperature for 1 h before observation using a PROVIS microscope with a Plan Apo 60×/1.40 oil ph3 objective and bright-field and appropriate filters (Olympus, Tokyo, Japan). The recording of the images was performed with an Olympus U-CMAD3 camera adapter and F-View II digital camera. The software used for recording images was analySIS Image Processing (Olympus). The exposure time for the bimolecular fluorescence complementation of YFP was 2 s for Mso1p–Sec1p and Mso1p–Sec4p(Q79L) and 5 s for Mso1p–Mso1p. Images were prepared using CorelDRAWX4 software (Corel, Mountain View, CA).

Bacterial production of Mso1p

N-terminally tagged, full-length Mso1p and N- and C-terminal fragments were produced in BL21 *Escherichia coli* cells. Expression was induced overnight with 0.2 mM isopropyl-β-D-thiogalactoside at 18°C, after which cells were collected and resuspended in 20 mM Tris-HCl, pH 8.0, and 0.4 mM phenylmethylsulfonyl fluoride. After addition of Triton X-100 to a final concentration of 0.5%, the cells were kept on ice for 10 min and sonicated. NaCl was added to a final concentration of 0.5 M, after which the lysates were centrifuged (10 min at 12,000 rpm, 4°C), and the N-terminally tagged Mso1p was purified from the supernatant using His-TrapFF column

(GE Healthcare, Piscataway, NJ). The tag alone and Mso1p fragments were produced in the same way. The concentrations of the purified proteins were measured by spectrophotometer using their calculated extinction coefficients at 280 nm.

Ras-rescue assay

The Ras-rescue assay was performed essentially as described previously (Isakoff et al., 1998). The H3751 strain was used for the assay. The plasmid B3254 was used as positive control. Four individual colonies of each transformation were examined for growth at different temperatures.

Bgl2p secretion

The intracellular accumulation of Bgl2p was measured essentially as described previously (Harsay and Schekman, 2007). In brief, *exo70-38* cells expressing different Mso1p variants were grown to an OD of 0.3–0.6, split into two identical cultures, and shifted to 37°C for 3 h. Cells were collected, cell lysates were generated, and the accumulated Bgl2p was detected with anti-Bgl2p antibody by Western blotting.

Lipid species

DPH, N-Rh-PE, and N-NBD-PE were obtained from Invitrogen. POPC, POPE, POPS, and L-α-phosphatidylinositol 4,5-bisphosphate were purchased from Avanti Polar Lipids (Alabaster, AL). And other phosphoinositides were from Echelon Bioscience (Salt Lake City, Utah).

Vesicle cosedimentation assay

Lipids in desired concentrations were mixed, dried under a stream of nitrogen, and the lipid residue subsequently maintained under reduced pressure for at least 2 h. The dry lipids were then hydrated in 20 mM 4-(2-hydroxyethyl)-1-piperazineethanesulfonic acid (HEPES), pH 7.5, and 100 mM NaCl to yield multilamellar vesicles. To obtain unilamellar vesicles, vesicles were extruded through a polycarbonate filter (100-nm pore size) using a mini extruder (Avanti Polar Lipids). Proteins and liposomes were incubated at room temperature for 10 min and centrifuged at 100,000 rpm with a Beckman rotor (TLA 100) for 30 min. The lipid composition of the liposomes is POPC:POPE:POPS:PIP₂ (50:20:20:10). The final concentrations of Mso1p and liposomes were 3 and 500 μM, respectively, in 20 mM HEPES, pH 7.5, buffer (with or without NaCl). Equal proportions of supernatants and pellets were loaded onto SDS-PAGE, and after electrophoresis the gels were stained with Coomassie blue. The intensities of Mso1p bands were quantified with the Quantity One program (Bio-Rad, Hercules, CA).

Fluorescence anisotropy of DPH

DPH was included into liposomes at a 1/500 ratio. The lipid concentration used was 40 μM. Fluorescence anisotropy for DPH was measured with a PerkinElmer (Waltham, MA) LS 55 spectrometer with excitation at 360 nm and emission at 450 nm using 10-nm bandwidths. The lipid compositions of the liposomes are POPC:POPE:POPS:PIP₂ (50:20:20:10), POPC:POPE (80:20), and POPC:POPE:POPS (60:20:20).

Quenching of Trp by brominated phosphatidylcholines

The tryptophan residue was excited at 280 nm, and emission spectra were recorded from 300 to 420 nm, averaging three scans. Spectra were corrected for the contribution of light scattering in the presence of vesicles. Collisional quenching of Trp-16 by brominated phospholipids (Br₂-PCs) was introduced to assess the localization of

this residue in bilayers. The indicated liposomes with a final concentration of 150 μM were added to 0.3 μM protein solution in 20 mM HEPES, 100 mM NaCl, pH 7.5. The differences in the quenching of Trp fluorescence by (6,7)-, (9,10)-, and (11,12)-Br₂-PC were used to calculate the probability for location of the fluorophore in the membrane using the parallax method (Chattopadhyay and London, 1987). The depth of the Trp residue was calculated from

$$Z_{cf} = L_{c1} + [-\ln(F_1/F_2)]/\pi C - L_{21}^2/2L_{21}$$

where Z_{cf} represents the distance of the fluorophore from the center of the bilayer, L_{c1} is the distance of the shallow quencher from the center of the bilayer, L_{21} is the distance between the shallow and the deep quencher, F_1 is the fluorescence intensity in the presence of the shallow quencher, F_2 is the fluorescence intensity in the presence of the deep quencher, and C is the concentration of quencher in molecules/ \AA^2 . Mso1p has two Trps, Trp-16 and Trp-69. However, only Trp-16 is involved in membrane penetration because the short N-terminal fragment 1–39 inserts into the lipid bilayer. The average bromine distances from the bilayer center, based on x-ray diffraction, were taken to be 10.8, 8.3, and 6.3 \AA for (6,7)-, (9,10)-, and (11,12)-Br₂-PC, respectively (Mcintosh and Holloway, 1987).

Light scattering assay

Intensity of 90° light scattering of the liposomes was monitored at 300 nm using the PerkinElmer LS 55 spectrofluorometer with both excitation and emission bandwidths set at 2.5 nm. Scattering intensity was measured continuously after the addition of 0.5 μM Mso1p. The lipid composition of the liposomes is POPC:POPE:PIPs (50:20:20:10), and the lipid concentration was 10 μM .

Fluorescence microscopy of mammalian PC6.3 cells

The neuron-like cell line PC6.3 was cultured in RPMI 1640 (Lonza, Basel, Switzerland) medium containing 2 mM L-glutamine, 10% horse serum, and 5% fetal bovine serum. For fluorescence microscopy the cells were grown on cover slides coated with polyornithine and laminin to ~70% confluence and transfected with the BiFC-, GFP-, or Cherry-tagged plasmids using Lipofectamine 2000 (Invitrogen, Carlsbad, CA). After 1 d of culturing, cells were fixed with 4% paraformaldehyde in phosphate-buffered saline. Fluorescence signals were observed using a Zeiss Axio Observer Z1 microscope with an ECPlanN 40x/0.75 DICII objective and Colibri laser (Carl Zeiss Imaging Solutions, Jena, Germany). Images were recorded with Zeiss Axio Vision, release 4.8.1, software. The exposure time for the bimolecular fluorescence complementation of Venus was 3 s, that of mCherry-Mint1 was 2 s, and that of GFP-PIP was 1–2 s. For quantification of the signal intensity original images obtained with the same microscope and the same exposure time were used. The BiFC interaction intensities were quantified using ImageJ 1.42 (National Institutes of Health, Bethesda, MD) by measuring the image mean gray value of equal-size boxes at the protrusion and in the cells body, followed by normalization of the protrusion BiFC signal to the cell-body BiFC signal. For each condition the signals in at least 25 cells were quantified. Image panels were prepared using Photoshop7 software (Adobe, San Jose, NJ).

ACKNOWLEDGMENTS

T. Balla, S. Emr, A. Gray, W. Guo, E. Harsay, D. Johnson, M. Knop, D. Lindholm, J. McNew, and P. Novick are acknowledged for kindly providing strains, plasmids, and/or antibodies. Anna-Liisa Nyfors is thanked for excellent technical assistance. Vesa Olkkonen is

acknowledged for cooperation. This work was financially supported by Academy of Finland Grants 124249 (J.J.), 123733 (N.A.), 121187 (H.Z.), 132988 (K.C.), and 137946 (P.L.), the Viikki Graduate School in Biosciences, the Helsinki Graduate Program in Biotechnology and Molecular Biology, the Magnus Ehrnrooth Foundation, the Alfred Kordelin Foundation, and the Institute of Biotechnology.

REFERENCES

- Aalto MK, Jantti J, Ostling J, Keranen S, Ronne H (1997). Mso1p: a yeast protein that functions in secretion and interacts physically and genetically with Sec1p. *Proc Natl Acad Sci USA* 94, 7331–7336.
- Carr CM, Rizo J (2010). At the junction of SNARE and SM protein function. *Curr Opin Cell Biol* 22, 488–495.
- Castillo-Flores A, Weinberger A, Robinson M, Gerst JE (2005). Mso1 is a novel component of the yeast exocytic SNARE complex. *J Biol Chem* 280, 34033–34041.
- Chattopadhyay A, London E (1987). Parallax method for direct measurement of membrane penetration depth utilizing fluorescence quenching by spin-labeled phospholipids. *Biochemistry* 26, 39–45.
- Di Paolo G, De Camilli P (2006). Phosphoinositides in cell regulation and membrane dynamics. *Nature* 443, 651–657.
- Harsay E, Schekman R (2007). Avl9p, a member of a novel protein superfamily, functions in the late secretory pathway. *Mol Biol Cell* 18, 1203–1219.
- He B, Guo W (2009). The exocyst complex in polarized exocytosis. *Curr Opin Cell Biol* 21, 537–542.
- He B, Xi FG, Zhang J, TerBush D, Zhang XY, Guo W (2007a). Exo70p mediates the secretion of specific exocytic vesicles at early stages of the cell cycle for polarized cell growth. *J Cell Biol* 176, 771–777.
- He B, Xi FG, Zhang XY, Zhang J, Guo W (2007b). Exo70 interacts with phospholipids and mediates the targeting of the exocyst to the plasma membrane. *EMBO J* 26, 4053–4065.
- Ho A, Liu XR, Sudhof TC (2008). Deletion of mint proteins decreases amyloid production in transgenic mouse models of Alzheimer's disease. *J Neurosci* 28, 14392–14400.
- Hu CD, Chinenov Y, Ranez-Carozzi VR, Grinberg AV, Kerppola TK (2002). gelfRET and BiFC: visualization of protein interactions in vitro and in living cells. *Biophys J* 82, 2A.
- Hutagalung AH, Novick PJ (2011). Role of Rab GTPases in membrane traffic and cell physiology. *Physiol Rev* 91, 119–149.
- Isakoff SJ, Cardozo T, Andreev J, Li Z, Ferguson KM, Abagyan R, Lemmon MA, Aronheim A, Skolnik EY (1998). Identification and analysis of PH domain-containing targets of phosphatidylinositol 3-kinase using a novel in vivo assay in yeast. *EMBO J* 17, 5374–5387.
- Jahn R, Scheller RH (2006). SNAREs—engines for membrane fusion. *Nat Rev Mol Cell Biol* 7, 631–643.
- Jantti J, Aalto MK, Oyen M, Sundqvist L, Keranen S, Ronne H (2002). Characterization of temperature-sensitive mutations in the yeast syntaxin 1 homologues Sso1p and Sso2p, and evidence of a distinct function for Sso1p in sporulation. *J Cell Sci* 115, 409–420.
- Kauppi M, Jantti J, Olkkonen VM (2004). The function of Sec1/Munc18 proteins—solution of the mystery in sight? In: *Regulatory Mechanisms of Intracellular Membrane Transport*, ed. S Keränen and J Jantti, Berlin: Springer, 115–143.
- Knop M, Miller KJ, Mazza M, Feng DJ, Weber M, Keranen S, Jantti J (2005). Molecular interactions position Mso1p, a novel PTB domain homologue, in the interface of the exocyst complex and the exocytic SNARE machinery in yeast. *Mol Biol Cell* 16, 4543–4556.
- Knop M, Strasser K (2000). Role of the spindle pole body of yeast in mediating assembly of the prospore membrane during meiosis. *EMBO J* 19, 3657–3667.
- Lazar T, Scheglmann D, Gallwitz D (2002). A novel phospholipid-binding protein from the yeast *Saccharomyces cerevisiae* with dual binding specificities for the transport GTPase Ypt7p and the Sec 1-related Vps33p. *Eur J Cell Biol* 81, 635–646.
- Lee HY, Park JB, Jang HI, Chae YC, Kim JH, Kim SI, Suh PG, Ryu SH (2004). Munc-18-1 inhibits phospholipase D activity by direct interaction in an epidermal growth factor-reversible manner. *FASEB J* 18, C21.
- Maying P (2012). Phosphoinositides and vesicular membrane traffic. *Biochim Biophys Acta* 1821, 1104–1113.
- Mcintosh TJ, Holloway PW (1987). Determination of the depth of bromine atoms in bilayers formed from bromolipid probes. *Biochemistry* 26, 1783–1788.

- Morgera F, Sallah MR, Dubuke ML, Gandhi P, Brewer DN, Carr CM, Munson M (2012). Regulation of exocytosis by the exocyst subunit Sec6 and the SM protein Sec1. *Mol Biol Cell* 23, 337–346.
- Munson M, Bryant NJ (2009). A role for the syntaxin N-terminus. *Biochem J* 418, e1–e3.
- Okamoto M, Sudhof TC (1997). Mints, Munc18-interacting proteins in synaptic vesicle exocytosis. *J Biol Chem* 272, 31459–31464.
- Peterson MR, Burd CG, Emr SD (1999). Vac1p coordinates Rab and phosphatidylinositol 3-kinase signaling in Vps45p-dependent vesicle docking/fusion at the endosome. *Curr Biol* 9, 159–162.
- Rogelj B, Mitchell JC, Miller CCJ, McLoughlin DM (2006). The X11/Mint family of adaptor proteins. *Brain Res Rev* 52, 305–315.
- Saarikangas J, Zhao HX, Pykalainen A, Laurinmaki P, Mattila PK, Kinnunen PKJ, Butcher SJ, Lappalainen P (2009). Molecular mechanisms of membrane deformation by I-BAR domain proteins. *Curr Biol* 19, 95–107.
- Sherman F (1991). *Guide to Yeast Genetics and Molecular and Cell Biology*, San Diego, CA: Academic Press, 3–41.
- Sivaram MVS, Furgason MLM, Brewer DN, Munson M (2006). The structure of the exocyst subunit Sec6p defines a conserved architecture with diverse roles. *Nat Struct Mol Biol* 13, 555–556.
- Skarp KP, Zhao X, Weber M, Jantti J (2008). Use of bimolecular fluorescence complementation in yeast *Saccharomyces cerevisiae*. *Methods Mol Biol* 457, 165–175.
- Sollner T, Bennett MK, Whiteheart SW, Scheller RH, Rothman JE (1993). A protein assembly-disassembly pathway in-vitro that may correspond to sequential steps of synaptic vesicle docking, activation, and fusion. *Cell* 75, 409–418.
- Stefan CJ, Audhya A, Emr SD (2002). The yeast synaptojanin-like proteins control the cellular distribution of phosphatidylinositol (4,5)-bisphosphate. *Mol Biol Cell* 13, 542–557.
- Tall GG, Hama H, Dewald DB, Horazdovsky BF (1999). The phosphatidylinositol 3-phosphate binding protein Vac1p interacts with a Rab GTPase and a Sec1p homologue to facilitate vesicle-mediated vacuolar protein sorting. *Mol Biol Cell* 10, 1873–1889.
- Toonen RFG, Verhage M (2003). Vesicle trafficking: pleasure and pain from SM genes. *Trends Cell Biol* 13, 177–186.
- Verhage M, de Vries KJ, Roshol H, Burbach JP, Gispen WH, Sudhof TC (1997). DOC2 proteins in rat brain: complementary distribution and proposed function as vesicular adapter proteins in early stages of secretion. *Neuron* 18, 453–461.
- Weber M, Chernov K, Turakainen H, Wohlfahrt G, Pajunen M, Savilahti H, Jantti J (2010). Mso1p regulates membrane fusion through interactions with the putative N-peptide-binding area in Sec1p domain 1. *Mol Biol Cell* 21, 1362–1374.
- Weber-Boyvat M, Aro N, Chernov KG, Nyman T, Jantti J (2011). Sec1p and Mso1p C-terminal tails cooperate with the SNAREs and Sec4p in polarized exocytosis. *Mol Biol Cell* 22, 230–244.
- Weisman LS, Wickner W (1992). Molecular characterization of Vac1, a gene required for vacuole inheritance and vacuole protein sorting. *J Biol Chem* 267, 618–623.
- Wiederkehr A, De Craene JO, Ferro-Novick S, Novick P (2004). Functional specialization within a vesicle tethering complex: bypass of a subset of exocyst deletion mutants by Sec1p or Sec4p. *J Cell Biol* 167, 875–887.
- Zhang XY, Orlando K, He B, Xi FG, Zhang J, Zajac A, Guo W (2008). Membrane association and functional regulation of Sec3 by phospholipids and Cdc42. *J Cell Biol* 180, 145–158.
- Zhang ZT, Lee CH, Mandiyan V, Borg JP, Margolis B, Schlessinger J, Kuriyan J (1997). Sequence-specific recognition of the internalization motif of the Alzheimer's amyloid precursor protein by the X11 PTB domain. *EMBO J* 16, 6141–6150.
- Zhao HX, Hakala M, Lappalainen P (2010). ADF/cofilin binds phosphoinositides in a multivalent manner to act as a PIP(2)-density sensor. *Biophys J* 98, 2327–2336.